

LOW CYCLE FATIGUE BEHAVIOUR AND FATIGUE CRACK INITIATION IN MAR-M247 AT 700 °C

ŠULÁK Ivo¹, OBRTLÍK Karel¹, HRBÁČEK Karel²

¹*Institute of Physics of Materials of the CAS, Brno, Czech Republic, EU, sulak@ipm.cz*

²*PBS Velká Bíteš a.s, Czech Republic, EU*

Abstract

The second generation nickel-based superalloy MAR-M247 offers a satisfying combination of fatigue and creep properties and oxidation and corrosion resistance that are required for application at elevated temperatures in hostile environments. The microstructure consists mainly of the face centred cubic γ matrix and ordered γ' strengthening precipitates ($L1_2$ crystal structure). The present work focuses on low cycle fatigue (LCF) behaviour of polycrystalline nickel-based superalloy MAR-M247 at high temperature. LCF tests were conducted on cylindrical specimens in symmetrical push-pull cycle under strain control with constant total strain amplitude and strain rate at 700 °C in ambient air. Cyclic stress-strain curves and fatigue life curves in the representation of plastic strain amplitude vs. stress amplitude and stress amplitude vs. the number of cycles to failure, respective, were plotted and compared with data obtained on Inconel 713LC. Special attention is paid to the investigation of crack initiation in MAR-M247 during low cycle fatigue. Crack initiation sites were studied by means of scanning electron microscopy (SEM) in dual beam microscope TESCAN LYRA 3 XMU FESEM equipped with focus ion beam (FIB). Specimens' surface observations revealed the formation of pronounced surface relief indicating localisation of plastic deformation. Observations in transmission electron microscope (TEM) confirmed localisation of cyclic plastic deformation in persistent slip bands along $\{111\}$ slip planes. Fractographic analysis revealed fatigue crack initiation sites. Fatigue crack propagation in stage I was typical of smooth facets up to 500 μm long.

Keywords: Nickel-based superalloy, cyclic stress-strain curve, fatigue life, fatigue crack initiation, focus ion beam

1. INTRODUCTION

MAR-M247 was developed in the early 1970s at Martin Metals Corporation and it belongs to the second generation of cast polycrystalline nickel-based superalloys [1]. It offers a satisfying combination of fatigue and creep properties and oxidation and corrosion resistance that are required for application at elevated temperatures in hostile environments [1-9]. MAR-M247 is used as a key material for integral wheels and turbine rotor blades. The complex loading conditions prevailing during service of these components can be simplified and tested in laboratories. The high-temperature low cycle fatigue (LCF) tests simulate severe elastic-plastic deformations during the start-ups and shut-downs periods. The LCF tests are designed to cause failure after a relatively small number of cycles that can be divided into the number of cycles to fatigue crack initiation N_i and the number of cycles to fatigue crack propagation N_p [10]. The initiation of fatigue crack is generally connected with the surface. During cyclic loading, the internal dislocation structure changes and narrow persistent slip bands (PSBs) along preferential slip traces are formed [11]. A pronounced surface relief consisting of extrusions and intrusions is build up at the intersection of the PSB with the free surface [12, 13]. Surface relief has been studied since 1903 and there is still no consensus on the mechanisms of fatigue crack initiation within surface slip markings [10, 14, 15]. However, with an increase in temperature other degradation mechanisms becomes more effective in the fatigue crack initiation compared with those at the surface slip markings [2, 16].

In this article, we report the LCF behaviour of MAR-M247 superalloy fatigued at 700 °C in ambient air. Obtained data are compared with data on Inconel 713LC. Cyclic stress-strain curves and fatigue life curves in Basquin representation are presented. Special attention is paid to the investigation of fracture surface and surface relief in MAR-M247 to identify the fatigue crack initiation sites at elevated temperature. Dislocation arrangements observed in transmission electron microscope help to discuss fatigue crack initiation mechanisms.

2. EXPERIMENTAL DETAILS

2.1. Material

The polycrystalline superalloy MAR-M247 was supplied by PBS Velká Bíteš, a.s. Czech Republic in a form of net-shape cast rods. The nominal chemical composition of studied melt D54 is as follow: 0.15 C, 8.37 Cr, 9.91 Co, 9.92 W, 0.67 Mo, 5.42 Al, 1.01 Ti, 3.05 Ta, 0.04 Fe, 0.015 B and 1.5 Hf, the rest is Ni (all in wt. %). Rods were hot isostatically pressed (1200 °C / 100 MPa / 4 h) in order to heal casting defects and thus prolong fatigue life [17]. Two steps heat treatment consisting of solid solution annealing at 1200 °C for 2h and subsequent precipitation hardening at 870 °C for 24 h was applied with the aim to get optimal microstructure. The superalloy MAR-M247 is characterised by coarse dendritic grains. The average grain size was 2.3 mm ± 0.4 mm. The microstructure consists of γ matrix channels, γ' strengthening phase in the form of coarse complex-shaped precipitates, fine cubic-shaped precipitates, rounded precipitates and γ/γ' eutectics. Carbide particles were randomly distributed both at grain boundaries and in interdendritic areas inside grains. The representative image of the microstructure of MAR-M247 is given in **Figure 1**. More details on the microstructure of MAR-M247 can be found elsewhere [2, 3, 18].

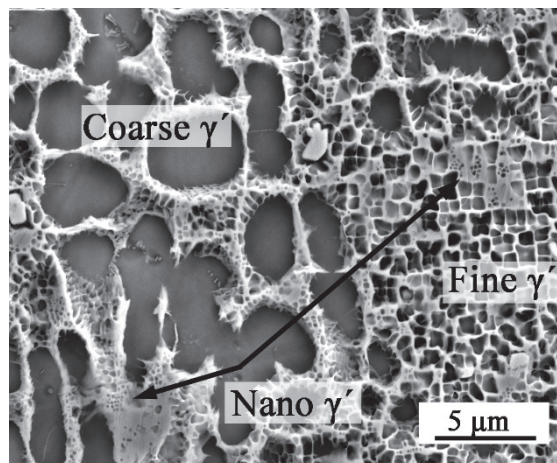


Figure 1 Microstructure of MAR-M247 showing the tri-modal morphology of γ' strengthening precipitates

2.2. Fatigue tests

LCF tests were performed on button-end cylindrical specimens with diameter, gauge length and gauge length roughness of 6 mm, 15 mm and 0.4 μm , respectively. They were carried out in a computer controlled electrohydraulic testing machine MTS 810 under strain control mode in a fully reversed pull-push cycle ($R_\epsilon = -1$) at 900°C in air. The strain rate ($2 \times 10^{-3} \text{ s}^{-1}$) and total strain amplitude were kept constant. The plastic strain amplitude ϵ_{ap} derived from the half of the hysteresis loop width at the mean stress σ_m and stress amplitude σ_a both at half-life were evaluated with a special program using recorded hysteresis loops. The number of cycles to failure N_f was defined as the number of elapsed cycles when the criterion $\sigma_m/\sigma_a \leq -0.3$ was met, or at the time of fracture before the criterion was reached. The heating was provided by the three-zone resistance furnace. The temperature was controlled by three thermocouples and one thermocouple was used to monitor the temperature. A temperature gradient within gauge length was $\pm 1^\circ\text{C}$.

2.3. Observations

The electrolytically polished gauge lengths and fracture surfaces of fatigued specimens representing the whole range of fatigue life were observed using a fully PC controlled dual beam SEM with Schottky field emission cathode TESCAN LYRA 3 XMU. SEM was equipped with focus ion beam (FIB) that was used to investigate details of fatigue crack initiation. Thin foils were observed in transmission electron microscope Philips CM12 STEM with a special focus on dislocation arrangement.

3. RESULTS AND DISCUSSION

3.1. Fatigue tests

Experimental data on cyclic stress-strain response and fatigue life obtained from LCF test are plotted in **Figure 2** and compared to data of Inconel 713LC [19]. Nominal composition of alloy 713LC is in **Table 1**.

Table 1 Nominal chemical composition of the alloy Inconel 713LC by TMS (wt.%)

Alloy	Ni	Cr	Mo	Al	Ti	Zr	Nb	C	B
Inconel 715LC	bal.	12	4.3	5.8	0.7	0.06	2	0.06	0.007

The representation of the stress amplitude vs. the plastic strain amplitude at half-life for both materials is shown in **Figure 2a** and yields the cyclic stress-strain curves (CSSCs). The stress-strain response of both materials is similar at low amplitudes and differs at high amplitudes. The shift to higher stress amplitudes can be explained by the higher strength of MAR-M247. On the other hand, the increase in plasticity of MAR-M247 in high total strain amplitude domain is considerably lower according to Inconel 713LC. Experimental data were fitted by the power law:

$$\log \sigma_a = \log K' + n' \log \varepsilon_{ap} \tag{1}$$

The parameters were evaluated using regression analysis and fatigue hardening coefficient K' is equal to 3200 (2090) and fatigue hardening exponent n' is 0.175 (0.137) for MAR-M247 (Inconel 713LC) superalloy.

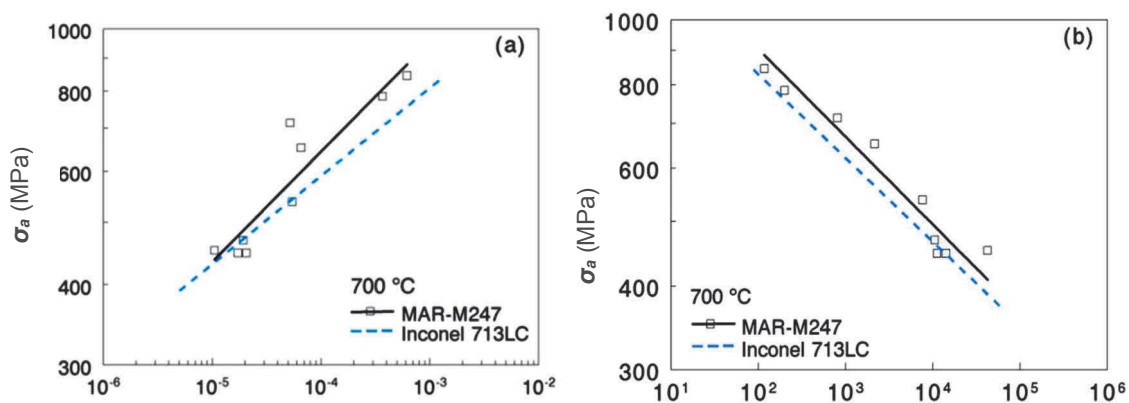


Figure 2 (a) Cyclic stress-strain curves; **(b)** Basquin fatigue life curves of MAR-M247 and Inconel 713LC

Fatigue life curves in the representation of the stress amplitude σ_a at half-life vs. the number of cycles to failure N_f are shown in **Figure 2b**. Experimental data were fitted by the Basquin law:

$$\log 2 N_f = (1/b) \log \sigma_a - (1/b) \log \sigma'_f \tag{2}$$

Fatigue strength coefficient σ'_f and fatigue strength exponent b were evaluated using regression analysis and for MAR-M247 (Inconel 713LC) superalloy are equal to 1810 MPa (1570 MPa) and -0.131 (-0.131), respectively. **Figure 2b** shows a slight increase in the fatigue life of MAR-M247 in the whole range of strain amplitudes. The increase can be attributed to the different chemical composition of MAR-M247 and Inconel 713LC [3]. According to Inconel 713LC, MAR-M247 contains W and Co that improve solid solution strengthening and an addition of Ta and Hf stabilise γ' precipitates against high-temperature degradation of MAR-M247 [3, 9].

3.2. Surface relief

After high-temperature LCF tests, surface relief was hindered by thin oxide scale. However, detailed inspection brought to light fatigue crack initiation sites mainly at oxidised carbides and grain boundaries (not shown here). This is in a good agreement with other studies that have been performed on MAR-M247 at different temperatures [2, 3]. Surface topography of a specimen fatigued to failure with total strain amplitude $\epsilon_a = 0.23$ % at 700 °C is shown in **Figure 3**. Pronounced surface relief of long and narrow surface slip markings going at the angle of 45° to the loading axis is present in **Figure 3a**. Slip markings witness the cyclic plastic strain localisation in individual grains of MAR-M247. In order to find evidence of fatigue crack initiation from slip markings, several FIB cuts have been made. **Figure 3b** illustrates FIB cut across slip markings and shows a deformed underlying structure and thin microcracks originated from slip markings as indicated in detail in left upper corner.

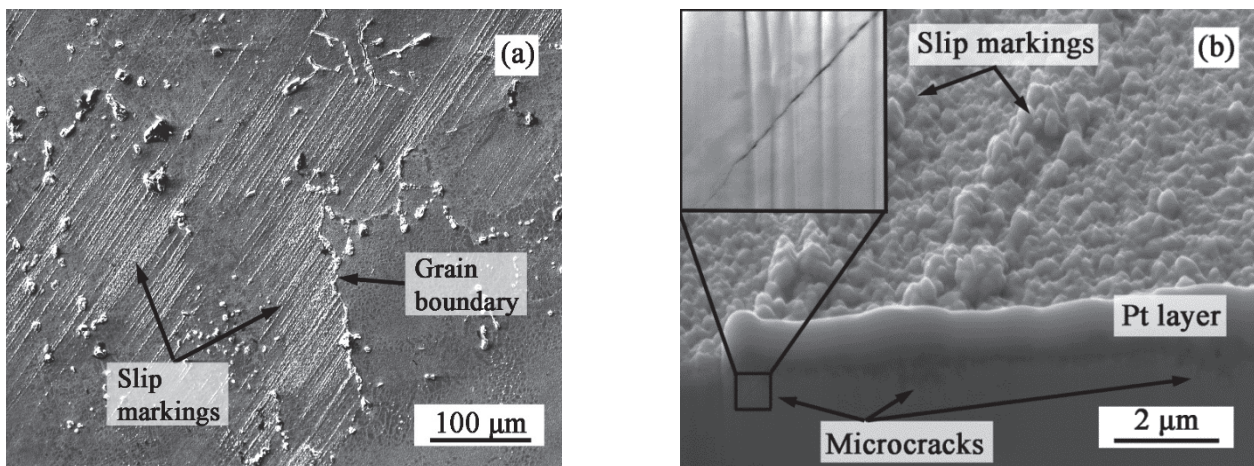


Figure 3 (a) Surface relief of MAR-M247; (b) FIB cut across slip markings

3.3. Dislocation structure

An example of inhomogeneous dislocation arrangement in a specimen cycled to failure ($\epsilon_a = 0.46$ %) is shown in **Figure 4**. The grain orientation $[1\bar{1}6\ 10]$ is denoted within the embedded standard stereographic triangle. Planar slip bands parallel to the primary slip planes $(1\ 1\ \bar{1})$ were observed to pass through both γ' precipitates and γ matrix channels. The Schmid factor of the primary slip system $(1\ 1\ \bar{1})\ [1\bar{1}1]$ is equal to 0.486. The Schmid factor of secondary slip system $(1\bar{1}1)\ [110]$ is very close and is equal to 0.463. The slip bands were present as thin slabs of high dislocation density (**Figure 4b**). The thickness and spacing of dislocation rich bands correspond to the thickness and spacing of individual surface slip markings on the surface (**Figure 3**). Therefore, it can be concluded that the cyclic plastic strain is localised into persistent slip bands at 700 °C. These observations are in good agreement with studies on nickel-based superalloys at elevated temperatures [19-22].

3.4. Fracture surface

Figure 5a illustrates fracture surface of specimen fatigued with total strain amplitude $\epsilon_a = 0.46\%$. The fatigue crack initiated at the surface and fatigue crack propagation in the stage I was observed with typically smooth facets up to 500 μm long as a consequence of localisation of cyclic plastic strain. This corresponds well with the dislocation arrangement and surface relief formation shown in the previous sections. The stage I of fatigue crack propagation in stress control fatigue conditions in MAR-M247 superalloys has been reported earlier [4, 5, 23]. Typical low stacking fault energy of nickel-based superalloys support the planar nature of cyclic slip and consequently, fatigue cracks propagate along active slip planes. Such damage mechanism is dominant at temperatures below 800 °C and disappears with an increase in temperature [2, 4]. **Figure 5b** shows fracture surface of a specimen fatigued with $\epsilon_a = 0.23\%$. The fatigue crack initiates in the vicinity of casting defects. Subsequent crack propagation via striation mechanism in the stage II is indicated by black arrows in **Figure 5b**.

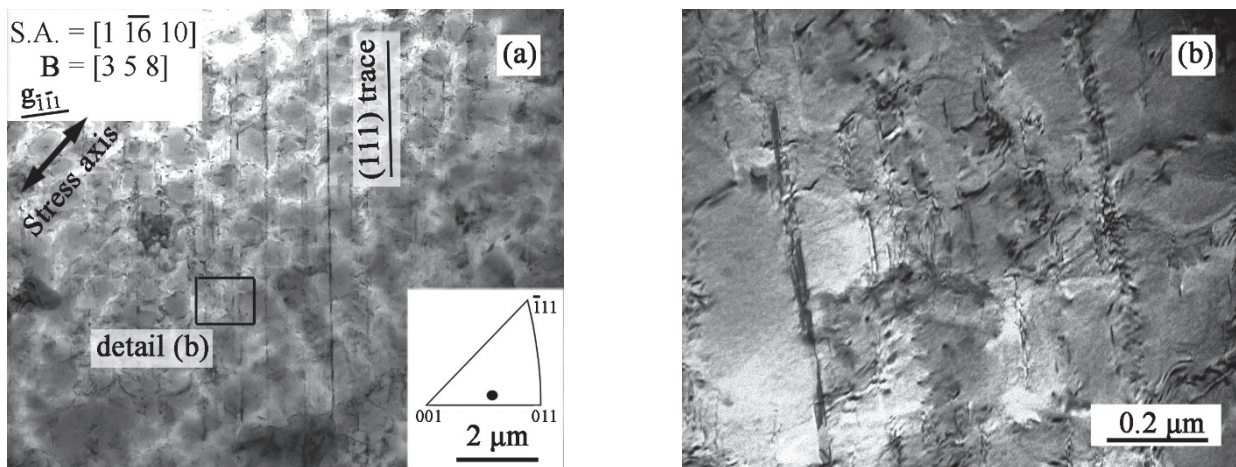


Figure 4 (a) TEM micrographs of specimen cycled to failure (S.A. is the stress axis) (b) detail of dislocation arrangement in persistent slip bands

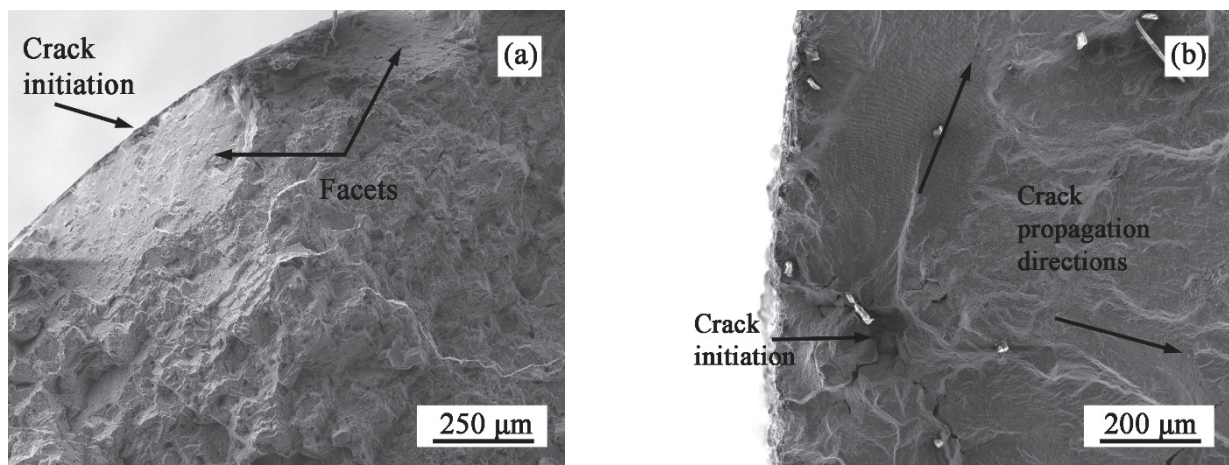


Figure 5 (a) Fatigue fracture surface with smooth facets (stage I) (b) fatigue crack initiation from casting defect and crack propagation in stage II

4. CONCLUSIONS

The following conclusions can be drawn from the study of fatigue behaviour and fatigue crack initiation in polycrystalline nickel-based superalloy MAR-M247 at 700°C in ambient air:

- 1) The stress response of MAR-M247 superalloy is similar to that of Inconel 713LC at low total strain amplitudes and becomes higher with the increase in strain amplitude compared to Inconel 713LC.

- 2) Basquin life curves confirmed the expectation of higher fatigue life of MAR-M247 compared to Inconel 713LC at 700 °C.
- 3) Grain boundaries, interdendritic areas, carbide particles and casting defects have been identified as important fatigue crack initiation sites at elevated temperature.
- 4) Strain localisation in persistent slip bands lying along {111} slip planes results in the formation of pronounced surface relief and in fatigue crack initiation at surface slip markings.
- 5) Smooth facets of the crystallographic crack growth (stage I) and the stage II non-crystallographic fatigue crack propagation through striation mechanism were observed.

ACKNOWLEDGEMENTS

The present research was financially supported by the grant No. 15-20991S of the Czech Science Foundation (GACR) and by the grant No. TA04011525 of the Technology Agency of the Czech Republic (TACR).

REFERENCES

- [1] HARRIS, K., ERICKSON, G. L., SCHWER, R. E. MAR M 247 derivations - CM 247 LC DS alloy CMSX single crystal alloys properties & performance. In *Proceedings of 5th International Symposium on Superalloys*, 1984, pp. 221-230.
- [2] ŠULÁK, I., OBRTLÍK, K., ČELKO, L. High-temperature low-cycle fatigue behaviour of HIP treated and untreated superalloy MAR-M247, *Kovové Materiály-Metallic Materials*, 2016, vol. 54, no. 6, pp. 471-481.
- [3] ŠULÁK, I., OBRTLÍK, K., ČELKO, L. Comparative study of microstructure and high temperature low cycle fatigue behaviour of nickel base superalloys Inconel 713LC and MAR-M247. *Key Engineering Materials*, 2016, vol. 713, pp. 86-89.
- [4] ŠMÍD, M., KUNZ, L., HUTAŘ, P., HRBÁČEK, K. High cycle fatigue of nickel-based superalloy MAR-M 247 at high temperatures. *Procedia Engineering*, 2014, vol. 74, pp. 329-332.
- [5] ŠMÍD, M., HORNÍK, V., HUTAŘ, P., HRBÁČEK, K., KUNZ, L. High cycle fatigue damage mechanisms of MAR-M 247 superalloy at high temperatures. *Transaction of Indian Institute of Metals*, 2016, vol. 69, pp. 393-397.
- [6] GUTH, S., DOLL, S., LANG, K. H. Lifetime, cyclic deformation and damage behaviour of MARM247 LC under thermo-mechanical fatigue loading with 0°, 180°, -90° and +90° phase shift between strain and temperature. *Procedia Engineering*, 2014, vol. 74, pp. 269-272.
- [7] BOISMIER, D. A., SEHITOGLU, H. Thermo-mechanical fatigue of Mar-M247. Part 1. Experiments, *Journal of Engineering Materials and Technology*, 1990, vol. 112, pp. 68-79.
- [8] BOR, H. Y., CHAO, C. G., MA, C. Y. The influence of magnesium on carbide characteristics and creep behavior of the Mar-M247 superalloy. *Scripta Materialia*, 1997, vol. 38, pp. 329-335.
- [9] REED, R. C. *The Superalloys: Fundamentals and Applications*. 1 edition, Cambridge University Press, Cambridge, UK; New York, 2008. 392 p.
- [10] SANGID, M. D. The physics of fatigue crack initiation. *International Journal of Fatigue*, 2013, vol. 57, pp. 58-72.
- [11] BUQUE, C. Persistent slip bands in cyclically deformed nickel polycrystals. *International Journal of Fatigue*, 2001, vol. 23, pp. 459-466.
- [12] POLÁK, J., PETRENEC, M., MAN, J. Dislocation structure and surface relief in fatigued metals. *Materials Science and Engineering A*, 2005, vols. 400-401, pp. 405-408.
- [13] POLÁK, J., PETRÁŠ, R., CHAI, G., ŠKORÍK, V. Surface profile evolution and fatigue crack initiation in Sanicro 25 steel at room temperature. *Materials Science and Engineering A*, 2016, vol. 658, pp. 221-228.
- [14] POLÁK, J., MAN, J. Experimental evidence and physical models of fatigue crack initiation. *International Journal of Fatigue*, 2016, vol. 91, pp. 294-303.
- [15] MUGHRABI, H. Cyclic slip irreversibilities and the evolution of fatigue damage. *Metallurgical and Materials Transactions A*. 2009, vol. 40, pp. 1257-1279.

- [16] PINEAU, A., ANTOLOVICH, S. D. High temperature fatigue of nickel-base superalloys - A review with special emphasis on deformation modes and oxidation. *Engineering Failure Analysis*, 2009, vol. 16, pp. 2668-2697.
- [17] ŠULÁK, I., OBRTLÍK, K., ŠKORÍK, V., HRBÁČEK, K. Effect of HIP on low cycle fatigue of MAR-M247 at 900°C. In METAL 2014: 23rd International Conference on Metallurgy and Materials. Ostrava: TANGER, 2014, pp. 1381-1386.
- [18] SZCZOTOK, A., RODAK, K. Microstructural studies of carbides in MAR-M247 nickel-based superalloy, In *IOP Conference Series, Materials Science and Engineering*, 2012, vol. 35. pp. 1-11.
- [19] PETRENEC, M., OBRTLÍK, K., POLÁK, J. High temperature low cycle fatigue of superalloys Inconel 713LC and Inconel 792-5A. *Key Engineering Materials*, 2007, vols. 348-349, pp. 101-104.
- [20] POLÁK, J., OBRTLÍK, K., PETRENEC, M., MAN, J., KRUML, T. Mechanisms of high temperature damage in elastoplastic cyclic loading of nickel superalloys and TiAl intermetallics. *Procedia Engineering*, 2013, vol. 55, pp. 114-122.
- [21] OBRTLÍK, K., PETRENEC, M., MAN, J., POLÁK, J., HRBÁČEK, K. Isothermal fatigue behavior of cast superalloy Inconel 792-5A at 23 and 900 °C. *Journal of Materials Science*, 2009, vol. 44, pp. 3305-3314.
- [22] PETRENEC, M., OBRTLÍK, K., POLÁK, J. Inhomogeneous dislocation structure in fatigued INCONEL 713 LC superalloy at room and elevated temperatures, *Materials Science Engineering A*. 2005, vols. 400-401, pp. 485-488.
- [23] HORNÍK, V., ŠMÍD, M., HUTAŘ, P., KUNZ, L., HRBÁČEK, K. Interaction of creep and high cycle fatigue of IN 713LC superalloy. *Solid State Phenomena*. 2017, vol. 258, pp. 595-598.